

Relevance of heat flux to correlation in nonequilibrium steady states

Chun-Hui Wang(王春辉), Hao-Ran Hu(胡皓然), Lei Li(李磊), Jian Zou(邹健), Wu-Ming Liu(刘伍明)
Citation: Chin. Phys. B. 35, 090302 (2026). DOI: 10.1088/1674-1056/ae1c2d |
CSTR: 32038.14.CPB.ae1c2d
http://cpb.iphy.ac.cn; http://iopscience.iop.org/cpb

What follows is a list of articles you may be interested in

Hierarchy of average correlation, quantum steering and Bell nonlocality in two-qubit systems

Qinglong Tian(田清龙), Youneng Guo(郭有能)
Chin. Phys. B. 35, 080302 (2026). DOI: 10.1088/1674-1056/ae6b38 | CSTR: 32038.14.CPB.ae6b38

Probing dephasing and non-Markovian effects on three-qubit states

Muhammad Noman, Aqsa Mushtaq, Wei Cui(崔巍)
Chin. Phys. B. 35, 050302 (2026). DOI: 10.1088/1674-1056/ae1822 | CSTR: 32038.14.CPB.ae1822

Dynamical evolution of imaginarity resources in non-Markovian environments

Hong-Biao Li(李宏彪), Deng-Guo Kong(孔德国), Xue-Ping Chai(柴学平), Jin-Long Yu(余金龙), Qiang Zheng(郑强)
Chin. Phys. B. 34, 110309 (2025). DOI: 10.1088/1674-1056/ade4b1 | CSTR: 32038.14.CPB.ade4b1

Observation of topology of non-Hermitian systems without chiral symmetry

Shuo Wang(王硕), Zhengjie Kang(康正杰), Hao Li(李浩), Jiaojiao Li(李姣姣), Yuanjie Zhang(张元杰), Zhihuang Luo(罗智煌)
Chin. Phys. B. 34, 110304 (2025). DOI: 10.1088/1674-1056/addcc1 | CSTR: 32038.14.CPB.addcc1

Machine learning of chaotic characteristics in classical nonlinear dynamics using variational quantum circuit

Sheng-Chen Bai(白生辰), Shi-Ju Ran(冉仕举)

Relevance of heat flux to correlation in nonequilibrium steady states

Chun-Hui Wang(王春辉)[1], Hao-Ran Hu(胡皓然)[1], Lei Li(李磊)[1,†], Jian Zou(邹健)[2,‡], and Wu-Ming Liu(刘伍明)[3,§]

[1] *Center for Quantum Physics and Technologies, School of Physical Science and Technology, Inner Mongolia University, Hohhot* 010021, *China*
[2] *School of Physics, Beijing Institute of Technology, Beijing* 100081, *China*
[3] *Institute of Physics, Chinese Academy of Sciences, Beijing* 100190, *China*

(Received 2 August 2025; revised manuscript received 22 October 2025; accepted manuscript online 6 November 2025)

We investigate the relation between heat flux and correlation in nonequilibrium steady states (NESSs), especially considering environmental memory effects. We construct a non-Markovian heat transport model using the repeated interactions scheme. The central system consists of system $\mathcal{S}$ and two memory qubits, coupled to heat reservoirs with different temperatures. The baths are modeled by sequences of ancilla qubits interacting with the central system. We prove that correlation between the central system and ancillas of the reservoir can witness the steady heat flux in the weak-coupling limit, and this consistency holds for heat flow presenting rectification behavior. This theoretical result can be confirmed numerically if and only if the coupling is weak. Furthermore, the non-Markovianity can impact the monotonicity of steady heat flux in the weak-coupling case, and the maximum value of heat current is at the boundary of Markovian and non-Markovian. Our results can be significant for heat management in hybrid open quantum systems or solid-state thermal circuits.

Keywords: non-equilibrium quantum thermodynamics, heat flux, correlation, quantum non-Markovianity, thermal rectification

PACS: 03.65.Yz, 03.65.Ta, 03.67.–a

DOI: 10.1088/1674-1056/ae1c2d **CSTR:** 32038.14.CPB.ae1c2d

1. Introduction

Although the field of equilibrium quantum thermodynamics is well established,[1,2] nonequilibrium thermodynamics is rapidly developing.[3–7] A fundamental thermodynamic quantity is the amount of energy that can be extracted from nonequilibrium systems. Work and heat are two fundamental physical quantities in quantum thermodynamics. Commonly, work is analyzed in the presence of external coherent control on the system,[8–10] while heat is due to some system–bath interaction that is associated with energy changes.[11–13] The role of correlation in mechanisms of energy exchange has attracted particular attention in recent years.[14–17] A representative example is the effect of correlation on the thermodynamic arrow of time, and it has been revealed that correlation can lead to reversal of the direction of heat flow from cold to hot.[18–20] Recently, consecutive interactions between individual elements of a quantum multipartite system and their own local environments have been investigated.[21–25] By studying these correlated channels, interesting new properties of quantum systems have been found in the presence of correlations. For example, Lorenzo *et al.* investigated heat flux and quantum correlations in dissipative cascaded systems and showed that the presence of initial correlations of the system can considerably affect the heat-flux rate.[26] Moreover, they found that the efficiency of the erasure process can be linked to the intrasystem correlations arising in the open dynamics of a multipartite system.[27] Pezzutto *et al.* studied the dynamics of a qubit system interacting with a multi-qubit environment, and they observed a synchronous behaviour between the emergence of non-Markovianity in the dynamics, the establishment of system–environment correlations, and violations of the Landauer bound.[28] In Ref. [29], the role of intraenvironmental correlation in open-system entropy production has been studied.

Quantum memory effects in the nonequilibrium steady state (NESS) have recently been considered in open quantum many-body systems. Purkayastha *et al.* have developed a general formalism that allows access to a full non-Markovian dynamics of open quantum many-body systems up to NESS.[30] Ask *et al.* have shown that an open quantum system in a non-Markovian environment can reach steady states that it cannot reach in a Markovian environment.[31] Heineken *et al.* have investigated dissipative preparation of entangled NESS, and they showed that memory effects can play an important role in the buildup of quantum correlations in NESS.[32] Motivated by this, in this work we study the impact of such memory effects on the nonlinear heat transport in the NESS. Meanwhile, there has been recent experimental investigation of superconducting quantum circuits[33,34] that validate long-standing theoret-

†Corresponding author. E-mail: lilei@imu.edu.cn
‡Corresponding author. E-mail: zoujian@bit.edu.cn
§Corresponding author. E-mail: wmliu@iphy.ac.cn

© 2026 Chinese Physical Society and IOP Publishing Ltd. All rights, including for text and data mining, AI training, and similar technologies, are reserved.

ical models of quantum heat transport,[35,36] and we contribute with a fundamental and insightful understanding of heat current and rectification in such models.

One way to prepare a NESS is to couple a central quantum system to two thermal baths with differing temperatures. Due to the temperature difference of the thermal baths, a typical characteristic of the NESS is a persistent heat current through the central system.[37–39] We investigate such a scenario by coupling a central quantum system, consisting of a qubit system and two memory qubits, to a hot and a cold thermal reservoir. We use a collision model approach,[40,41] also known as the repeated interactions scheme, of quantum thermodynamics.[42–44] One growing field of applications is quantum transport phenomena, which also include energy transport due to heat currents.[45–47] Furthermore, collision models provide an approach for describing the dynamics of system-environment correlations,[48–51] which is essential for the understanding of non-Markovian quantum dynamics.[52–54]

The outline of the paper is as follows. In Section 2, we describe the model under consideration. In Section 3, we focus on the relevance of correlation between the central quantum system and ancillas of reservoir to heat flux of the NESS. Non-Markovianity and thermal rectification are discussed in Section 4. Finally, in Section 5, we draw our conclusions.

2. Model

We consider a single-qubit system $\mathcal{S}$ with Hamiltonian $\hat{H}_{\mathcal{S}} = \omega\hat{\sigma}_z/2$ which couples to two hierarchical environments, ω and $\hat{\sigma}_z$ are the transition frequency and the Pauli matrices, respectively, and we set $\hbar = 1$ throughout this paper. Each hierarchical environment contains a memory qubit $\mathcal{A}_{h(c)}$ and a reservoir $\mathcal{R}_{h(c)}$ consisting of a large collection of N identical noninteracting ancillas (qubits) $\{\mathcal{R}_1^{h(c)}, \mathcal{R}_2^{h(c)}, \ldots, \mathcal{R}_N^{h(c)}\}$ (see Fig. 1). The two environments are initially in the product state $\rho_{E_h} = \rho_{\mathcal{A}_h} \otimes_{j=1}^{N} \eta_j^h$ and $\rho_{E_c} = \rho_{\mathcal{A}_c} \otimes_{j=1}^{N} \eta_j^c$, respectively. Each subenvironmental qubit, including two memory qubits and ancillas, is in the canonical thermal state $\rho_\beta^{h(c)} = \mathrm{e}^{-\beta_{h(c)}\hat{H}_{\mathrm{E}}}/Z_{h(c)}$. Here, $\beta_{h(c)} = 1/k_{\mathrm{B}}T_{h(c)}$ and $Z_{h(c)} = \mathrm{Tr}[\mathrm{e}^{-\beta_{h(c)}\hat{H}_{\mathrm{E}}}]$ are the corresponding inverse temperature and the partition function, respectively. $\hat{H}_{\mathrm{E}} = \omega\hat{\sigma}_z/2$ is the local Hamiltonian of each subenvironmental qubit. The evolution of system $\mathcal{S}$ and its interaction with the environments are as follows: $\mathcal{S}$ and two memory qubits interact first, subsequently $\mathcal{A}_h$ and $\mathcal{A}_c$ collide with the individual ancilla in $\mathcal{R}_h$ and $\mathcal{R}_c$, respectively, and then this process is repeated. The general scheme is illustrated in Fig. 1. The assumption of a large collection of ancillas implies that the memory qubit never interacts twice with the same ancilla, i.e., at each collision, the state of the ancilla is refreshed. This process is implemented through the unitary operator

$$\hat{U}_{\mathrm{tot}} = \hat{\mathcal{U}}_{\mathcal{A}_h,\mathcal{R}_j^h}\hat{\mathcal{U}}_{\mathcal{A}_c,\mathcal{R}_j^c}\hat{\mathcal{U}}_{\mathcal{S},\mathcal{A}_h}\hat{\mathcal{U}}_{\mathcal{S},\mathcal{A}_c}, \tag{1}$$

where $\hat{\mathcal{U}}_{\mathcal{S},\mathcal{A}_{h(c)}} = \mathrm{e}^{-\mathrm{i}\hat{H}_1^{\mathrm{int}}\tau}$, $\hat{\mathcal{U}}_{\mathcal{A}_{h(c)},\mathcal{R}_j^{h(c)}} = \mathrm{e}^{-\mathrm{i}\hat{H}_2^{\mathrm{int}}\tau}$. Here $\hat{H}_1^{\mathrm{int}}$ and $\hat{H}_2^{\mathrm{int}}$ are the interactions between $\mathcal{S}$ and $\mathcal{A}_{h(c)}$ and the interactions between $\mathcal{A}_{h(c)}$ and $\mathcal{R}_j^{h(c)}$, respectively, τ is the collision time. We consider a coherent interaction between the bipartite systems, $\hat{H}_{1(2)}^{\mathrm{int}} = g_{1(2)}(\hat{\sigma}_x\hat{\sigma}_x + \hat{\sigma}_y\hat{\sigma}_y + \hat{\sigma}_z\hat{\sigma}_z)$, with $g_{1(2)}$ being a coupling constant. In this case, we can write the unitary time-evolution operator $\hat{\mathcal{U}}_{\mathcal{S},\mathcal{A}_{h(c)}}$ in Eq. (1) as[55]

$$\hat{\mathcal{U}}_{\mathcal{S},\mathcal{A}_{h(c)}}(\gamma_{h(c)}) = (\cos\gamma_{h(c)})\hat{\mathbb{I}} + \mathrm{i}(\sin\gamma_{h(c)})\hat{S}_{\mathrm{sw}}, \tag{2}$$

where $\gamma_{h(c)} = 2g_1\tau$ is a dimensionless interaction strength, $\hat{\mathbb{I}}$ is the identity operator, and $\hat{S}_{\mathrm{sw}}$ is the two-particle swap operator whose action is $|\psi_1\rangle \otimes |\psi_2\rangle \to |\psi_2\rangle \otimes |\psi_1\rangle$ for all $|\psi_1\rangle, |\psi_2\rangle \in \mathbb{C}^2$. It is clear that $\gamma_{h(c)} = \pi/2$ induces a complete swap between the state of $\mathcal{S}$ and that of $\mathcal{A}_{h(c)}$. Thus, $0 < \gamma_{h(c)} < \pi/2$ means a partial swap, in effect, part of the information contained in the state of $\mathcal{S}$ is transferred into $\mathcal{A}_{h(c)}$ at each collision. In the ordered basis $\{|00\rangle, |01\rangle, |10\rangle, |11\rangle\}$ $\hat{S}_{\mathrm{sw}}$ reads[56]

$$\hat{S}_{\mathrm{sw}} = \begin{pmatrix} 1 & 0 & 0 & 0 \\ 0 & 0 & 1 & 0 \\ 0 & 1 & 0 & 0 \\ 0 & 0 & 0 & 1 \end{pmatrix}. \tag{3}$$

Similarly $\hat{\mathcal{U}}_{\mathcal{A}_{h(c)},\mathcal{R}_j^{h(c)}} = (\cos\delta_{h(c)})\hat{\mathbb{I}} + \mathrm{i}(\sin\delta_{h(c)})\hat{S}_{\mathrm{sw}}$, with $\delta_{h(c)} \neq \gamma_{h(c)}$ in general. As mentioned above, the dynamics of system $\mathcal{S}$ consists of sequential system–environment interaction interspersed with interenvironmental collisions. Thus, the evolution of a total system composed of a system and the environment during the $(n+1)$th interaction is

$$\rho_{n+1}^{\mathrm{tot}} \to \tilde{\rho}_{n+1}^{\mathrm{tot}} = \hat{U}_{\mathrm{tot}}\rho_{n+1}^{\mathrm{tot}}\hat{U}_{\mathrm{tot}}^{\dagger}, \tag{4}$$

where $\rho_{n+1}^{\mathrm{tot}} = \rho_n^{\mathcal{S}\mathcal{A}_h\mathcal{A}_c} \otimes \eta_{n+1}^h \otimes \eta_{n+1}^c$, and $\rho_n^{\mathcal{S}\mathcal{A}_h\mathcal{A}_c}$ is the state of the central system $\mathcal{S}\mathcal{A}_h\mathcal{A}_c$ (system + two memory qubits) after the nth interaction. Hence, after the $(n+1)$th interaction, the state of the $(n+1)$th ancilla of reservoir $\mathcal{R}_h$ ($\mathcal{R}_c$) is

$$\tilde{\eta}_{n+1}^{h(c)} = \mathrm{Tr}_x[\tilde{\rho}_{n+1}^{\mathrm{tot}}], \tag{5}$$

where $\mathrm{Tr}_x[\cdots]$ means the trace of $\mathcal{S}\mathcal{A}_h\mathcal{A}_c$ and $\mathcal{R}_{n+1}^{c(h)}$ degrees of freedom. And $\rho_{n+1}^{\mathcal{S}\mathcal{A}_h\mathcal{A}_c} = \mathrm{Tr}_{\mathcal{R}_{n+1}^h\mathcal{R}_{n+1}^c}[\tilde{\rho}_{n+1}^{\mathrm{tot}}]$, $\tilde{\eta}_{n+1}^{hc} = \mathrm{Tr}_{\mathcal{S}\mathcal{A}_h\mathcal{A}_c}[\tilde{\rho}_{n+1}^{\mathrm{tot}}]$. Note that $[\hat{\mathcal{U}}_{\mathcal{S},\mathcal{A}_c}, \hat{\mathcal{U}}_{\mathcal{S},\mathcal{A}_h}] \neq 0$, thus the cooling down and the heating up processes do not commute with each other. In this paper, we consider the steady-state properties of the system and we randomly designate the cooling process to occur first in Eq. (1).

We consider energy-conserving interactions, i.e., $[\hat{H}_1^{\mathrm{int}}, (\hat{H}_{\mathcal{S}} + \hat{H}_{\mathrm{E}})] = 0$, $[\hat{H}_2^{\mathrm{int}}, \hat{H}_{\mathrm{E}}] = 0$, thus we avoid subtleties of distinguishing heat from work because the latter vanishes in this case. From Eq. (5), we can obtain the heat exchange

between reservoir $\mathcal{R}_{h(c)}$ and memory qubit $\mathcal{A}_{h(c)}$ during the $(n+1)$th collision

$$\Delta Q_{n+1}^{\mathcal{R}^{h(c)}} = \mathrm{Tr}[\hat{H}_{\mathrm{E}}(\tilde{\eta}_{n+1}^{h(c)} - \eta_{n+1}^{h(c)})], \tag{6}$$

and in the steady regime

$$\Delta Q_{n+1}^{h} = -\Delta Q_{n+1}^{c}. \tag{7}$$

Therefore, Eq. (7) can also be defined as the steady-state heat current

$$J_{h(c)}^{\mathrm{ste}} = \Delta Q_{n+1}^{h(c)}, \tag{8}$$

i.e., the heat flows into (or out of) reservoir $\mathcal{R}_{h(c)}$ during the $(n+1)$th interaction.

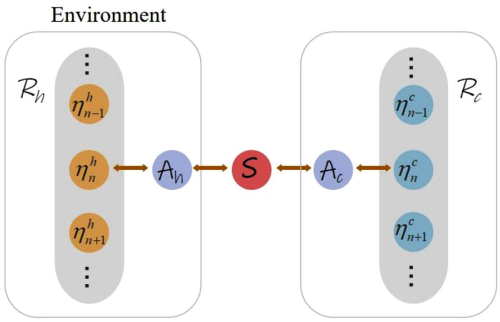


Fig. 1. Sketch of the protocol of system $\mathcal{S}$ plus two hierarchical environments. After $\mathcal{A}_h$ and $\mathcal{A}_c$ interact with $\mathcal{R}_n^h$ and $\mathcal{R}_n^c$, respectively, they collide with $\mathcal{S}$ and are then directed to the $(n+1)$th ancillas of two reservoirs.

3. Heat current and correlations

The change in entropy of the central system $\mathcal{SA}_h\mathcal{A}_c$ (system $\mathcal{S}$ + two memory qubits $\mathcal{A}_h\mathcal{A}_c$) during the $(n+1)$th interaction can be expressed as

$$\Delta S_{n+1} = S(\rho_{n+1}^{\mathcal{SA}_h\mathcal{A}_c}) - S(\rho_n^{\mathcal{SA}_h\mathcal{A}_c}). \tag{9}$$

In the weak coupling limit, $\delta_{h(c)} \to 0$ or $\gamma_{h(c)} \to 0$, $S(\tilde{\eta}_{n+1}^{hc}) \simeq \sum_i S(\tilde{\eta}_{n+1}^i)$, where $i = h, c$. Thus, Eq. (9) can be written as

$$\begin{aligned}\Delta S_{n+1} &= -S(\rho_n^{\mathcal{SA}_h\mathcal{A}_c}) + S(\rho_{n+1}^{\mathrm{tot}}) - \textstyle\sum_i S(\tilde{\eta}_{n+1}^i) \\ &\quad + I(\rho_{n+1}^{\mathcal{SA}_h\mathcal{A}_c}, \tilde{\eta}_{n+1}^{hc}) \\ &= \mathrm{Tr}[\rho_{n+1}^{\mathrm{tot}} \ln \rho_n^{\mathcal{SA}_h\mathcal{A}_c}] - \mathrm{Tr}[\rho_{n+1}^{\mathrm{tot}} \ln \rho_{n+1}^{\mathrm{tot}}] \\ &\quad + \sum_i \mathrm{Tr}[\tilde{\eta}_{n+1}^i \ln \tilde{\eta}_{n+1}^i] + I(\rho_{n+1}^{\mathcal{SA}_h\mathcal{A}_c}, \tilde{\eta}_{n+1}^{hc}),\end{aligned} \tag{10}$$

where $I(\rho_{n+1}^{\mathcal{SA}_h\mathcal{A}_c}, \tilde{\eta}_{n+1}^{hc})$ is the correlation established between central system $\mathcal{SA}_h\mathcal{A}_c$ and the ancillas during the $(n+1)$th interaction. Here, we use the mutual information to measure this correlation, which is defined as[57]

$$I(\rho_{\mathrm{A}}, \rho_{\mathrm{B}}) = S(\rho_{\mathrm{A}}) + S(\rho_{\mathrm{B}}) - S(\rho_{\mathrm{AB}}), \tag{11}$$

where $S(\rho) = -\mathrm{Tr}[\rho \ln \rho]$ is the von Neumann entropy. Following, we define a quantity ξ as

$$\begin{aligned}\xi &= \textstyle\sum_i \mathcal{D}(\tilde{\eta}_{n+1}^i \parallel \eta_{n+1}^i) \\ &= \textstyle\sum_i \mathrm{Tr}(\tilde{\eta}_{n+1}^i \ln \tilde{\eta}_{n+1}^i) - \mathrm{Tr}(\tilde{\eta}_{n+1}^i \ln \eta_{n+1}^i),\end{aligned} \tag{12}$$

where $\mathcal{D}(\rho_1 \parallel \rho_2) \equiv \mathrm{Tr}(\rho_1 \ln \rho_1) - \mathrm{Tr}(\rho_1 \ln \rho_2)$ is the quantum relative entropy between two density matrices ρ_1 and ρ_2. In addition, Eq. (10) can be rewritten as

$$\begin{aligned}\Delta S_{n+1} &= \textstyle\sum_i \mathrm{Tr}[(\tilde{\eta}_{n+1}^i - \eta_{n+1}^i) \ln \eta_{n+1}^i] \\ &\quad + I(\rho_{n+1}^{\mathcal{SA}_h\mathcal{A}_c}, \tilde{\eta}_{n+1}^{hc}) + \xi.\end{aligned} \tag{13}$$

Clearly, the first term on the right-hand side of Eq. (13) can be expressed as $-\sum_i \beta_i \Delta Q_{n+1}^i$, and Eq. (13) becomes

$$\Delta S_{n+1} = -\sum_i \beta_i \Delta Q_{n+1}^i + I(\rho_{n+1}^{\mathcal{SA}_h\mathcal{A}_c}, \tilde{\eta}_{n+1}^{hc}) + \xi. \tag{14}$$

Note that in the steady regime $\Delta S_{n+1} = 0$, and for negative temperature gradient, i.e., $T_h \geqslant T_c$, we obtain

$$(\beta_h - \beta_c) J_h^{\mathrm{ste}}(\Delta T) = I(\Delta T) + \xi(\Delta T), \tag{15}$$

with $\Delta T = |T_h - T_c|$. It can be shown that the steady-state heat current $J_h^{\mathrm{ste}}(\Delta T)$ and correlation $I(\Delta T)$ are maintained in Eq. (15) in the weak coupling limit, and actually $\xi(\Delta T)$ is a small perturbation. In the following, for convenience, we use the logogram $\{J_h^{\mathrm{ste}}, I, \xi\}$ to replace $\{J_h^{\mathrm{ste}}(\Delta T), I(\Delta T), \xi(\Delta T)\}$, and we study the relation between steady-state heat flux and correlation by numerical calculations.

In Fig. 2 we let $\gamma_h = \gamma_c = \gamma$ and $\delta_h = \delta_c = \delta$. We show the three terms $(\beta_h - \beta_c)J_h^{\mathrm{ste}}$, correlation I and ξ in Eq. (15) as a function of δ and γ in (a) and (c), respectively, which are the

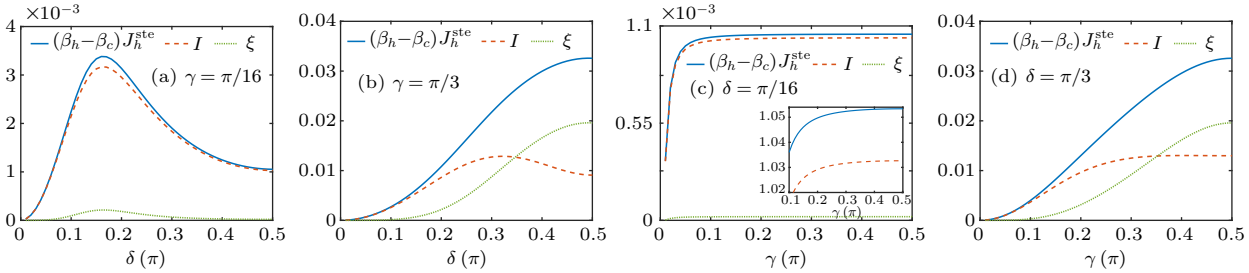


Fig. 2. The three terms $(\beta_h - \beta_c)J_h^{\mathrm{ste}}$, correlation I and ξ in Eq. (15) as a function of the coupling strength δ and γ. In (a) and (c), $\gamma = \pi/16$ and $\delta = \pi/16$, respectively, which are the weak-coupling regimes, and in (b) and (d), $\gamma = \pi/3$ and $\delta = \pi/3$, respectively, with a larger coupling. For all plots, we choose the ground state of system $|\psi\rangle_{\mathcal{S}} = |1\rangle$, $T_h = 2T_c = 2$ (i.e., $\beta_h = \frac{1}{2}\beta_c = \frac{1}{2}$) and $k_{\mathrm{B}} = \omega = 1$.

weak-coupling regimes with $\gamma = \pi/16$ (a) and $\delta = \pi/16$ (c). This shows that the behaviors of $(\beta_h - \beta_c)J_h^{\rm ste}$ and I are highly consistent in this weak-coupling case. Specifically, they are first enhanced and then decreased with the increase of δ for fixed γ, while they increase monotonously with the increase of γ for fixed δ, which can be seen more clearly from the inset of Fig. 2(c). This consistency of $(\beta_h - \beta_c)J_h^{\rm ste}$ and I happens because Eq. (15) is approximately true for the weak coupling case, and ξ plays a minor role in the contribution. However, the consistency is destroyed for a larger coupling, as shown in Figs. 2(b) and 2(d), where $\gamma = \pi/3$ and $\delta = \pi/3$, respectively. In order to obtain the range of the coupling that can realize the consistent behaviors between steady heat flux and correlation, we define

$$\mathcal{C}(\gamma)_\delta = \frac{2}{\pi}\int_0^{\frac{\pi}{2}} \delta_{ij}\mathrm{d}\gamma, \tag{16}$$

as a mathematical measure, where δ_{ij} is the Kronecker function with $i = \dot{J}_h^{\rm ste}(\gamma)/|\dot{J}_h^{\rm ste}(\gamma)|$ and $j = \ddot{I}(\gamma)/|\ddot{I}(\gamma)|$, i.e., $\delta_{ij} = 1$ if $i = j$ and $\delta_{ij} = 0$ if $i \neq j$; $\dot{J}_h^{\rm ste}(\gamma) = \frac{\mathrm{d}^2}{\mathrm{d}\gamma^2}J_h^{\rm ste}(\gamma)$ and $\ddot{I}(\gamma) = \frac{\mathrm{d}^2}{\mathrm{d}\gamma^2}I(\gamma)$, with fixed coupling strength δ. Similarly,

$$\mathcal{C}(\delta)_\gamma = \frac{2}{\pi}\int_0^{\frac{\pi}{2}} \delta_{\alpha\beta}\mathrm{d}\delta, \tag{17}$$

where $\delta_{\alpha\beta}$ is the Kronecker function, $\alpha = \dot{J}_h^{\rm ste}(\delta)/|\dot{J}_h^{\rm ste}(\delta)|$ and $\beta = \ddot{I}(\delta)/|\ddot{I}(\delta)|$, $\dot{J}_h^{\rm ste}(\delta) = \frac{\mathrm{d}^2}{\mathrm{d}\delta^2}J_h^{\rm ste}(\delta)$ and $\ddot{I}(\delta) = \frac{\mathrm{d}^2}{\mathrm{d}\delta^2}I(\delta)$, with fixed coupling strength γ. Note that $\mathcal{C}(\gamma)_\delta$ and $\mathcal{C}(\delta)_\gamma \in [0,1]$. When it reaches the maximum value 1, the monotonicity of $J_h^{\rm ste}$ and I are completely consistent. We calculate Eqs. (16) and (17) in Figs. 3(a) and 3(b), respectively. In (a), we go through the entire interval $\delta \in (0, \pi/2]$ with interval 0.01π for each value of the abscissa γ. Similarly, each value of the abscissa δ walks through the entire interval $\gamma \in (0, \pi/2]$ with interval 0.01π in (b). This shows that a perfect witness between the heat flux and correlation appears when the maximum value 1 is reached. From numerical calculation, this consistency is maintained in the range $\gamma \lesssim 0.13\pi$ or $\delta \lesssim 0.18\pi$, which is the weak-coupling case. The steady heat flux is witnessed by quantum correlation in this weak-coupling range.

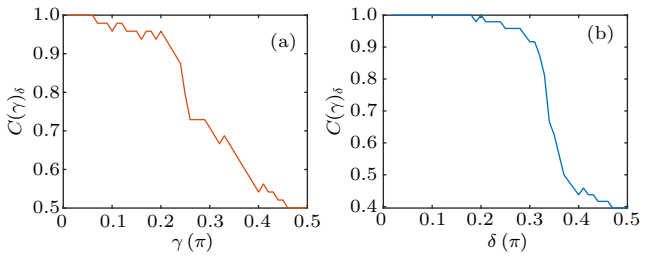


Fig. 3. The consistency between the steady-state heat flux and correlation as a function of the coupling strength γ and δ in (a) and (b), respectively. For all plots $|\psi\rangle_S = |1\rangle$, $T_h = 2T_c = 2$ and $k_B = \omega = 1$.

4. Non-Markovianity and thermal rectification

As mentioned above, for small fixed-coupling γ ($\gamma \lesssim 0.13\pi$), the behaviors of steady heat flux $J_h^{\rm ste}$ and correlation I are almost consistent with variate δ. Specifically, they increase and then decrease with the increase of δ, i.e., there exists a maximum value of $J_h^{\rm ste}$ (or I), as Fig. 2(a) shows. In Fig. 4, we plot the maximum value of $J_h^{\rm ste}$ as a function of two couplings γ and δ with temperature difference $\Delta T = 1$. Interestingly, this maximum is at the boundary of Markovian and non-Markovian when $\gamma \lesssim 0.13\pi$. Here, the blue stars represent the degree of non-Markovianity being equal to zero (Markovian) and the orange dots represent the degree of non-Markovianity being larger than zero (non-Markovian), and the maximum value of $J_h^{\rm ste}$ is shown by the red five-pointed star. From numerical calculations, we find that this correspondence does not depend on temperature difference ΔT. In other words, for small or large temperature difference the maximum value of $J_h^{\rm ste}$ also coincides with the boundary between the non-Markovian and Markovian regimes (for the full details, see Appendix A). Physically this can be understood as follows. In this weak-coupling interval $\gamma \lesssim 0.13\pi$, the behaviors of steady heat flux and correlation I are highly consistent with variate δ for a fixed γ; meanwhile, it undergoes a non-Markovian–Markovian transition with the increase of δ for fixed γ. For the first half of non-Markovian process, the correlation I is always increased and reaches the maximum at the critical point of non-Markovian and Markovian, it then decreases monotonously with the Markovian process. In this weak-coupling regime, we are concerned that the correlation I and heat flux can witness each other, which leads to the drop point of maximum $J_h^{\rm ste}$ at the boundary of Markovian and non-Markovian. In contrast, for small fixed-coupling δ, it undergoes a quick transition from Markov to non-Markov processes with the increase of γ (see Fig. 4). Therefore, the correlation I (or heat flux) is enhanced rapidly, which corresponds to the transition from Markovian regime to non-Markovian case, and then increases constantly with the increase of γ in the

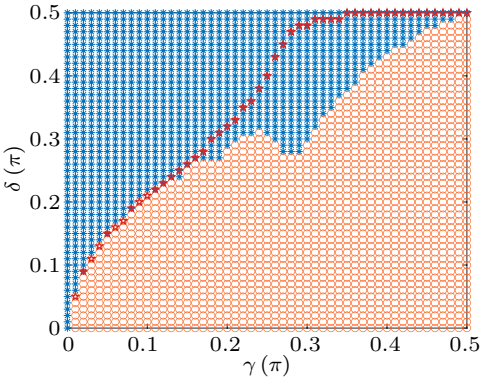


Fig. 4. Markovian region shown by the blue stars, the non-Markovian region presented by the orange dots, and the maximum value of the steady heat flux with red five-pointed star, against the coupling strength γ and δ. The initial state of system is $|\psi\rangle_S = |1\rangle$, $T_h = 2T_c = 2$ and $k_B = \omega = 1$.

non-Markovian regime, as shown in Fig. 2(c). Through the above discussion, we can see that the steady heat flux (or correlation) increases with δ monotonically for small fixed γ in non-Markovian region, which decreases with δ monotonically in Markovian region. In other words, in the weak-coupling case, we observe a monotonic behavior of the steady heat flux or correlation. Its monotonicity is closely related to whether the dynamical process is non-Markovian or not.

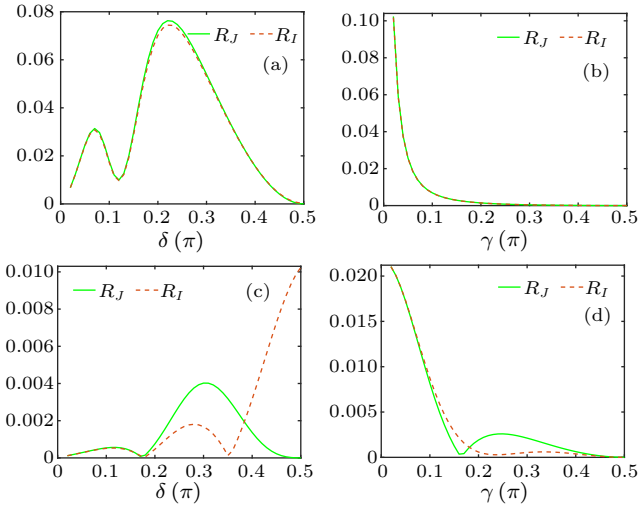


Fig. 5. The steady-state rectification factor R_J and correlation-relevant quantity R_I as a function of the coupling strength δ and γ. (a) $\gamma_h = \pi/16$ and $\gamma_c = \pi/32$, and (b) $\delta_h = \pi/16$ and $\delta_c = \pi/32$, both are the weak-coupling case. (c) $\gamma_h = \pi/3$ and $\gamma_c = \pi/4$, and (d) $\delta_h = \pi/3$ and $\delta_c = \pi/4$, with a larger coupling. For all plots, $|\psi\rangle_{\mathcal{S}} = |1\rangle$, $T_h = 2T_c = 2$ and $k_{\rm B} = \omega = 1$.

As a figure of merit to assess possible thermal rectification performance, we first adopt the so-called rectification coefficient defined as follows:[58–60]

$$R_J = \frac{|J_h(\Delta T) + J_h(-\Delta T)|}{\max(|(J_h(\Delta T)|, |J_h(-\Delta T)|)}, \tag{18}$$

where $J_h(\Delta T)$ is the forward heat current for $T_h \geqslant T_c$, and $J_h(-\Delta T)$ is the backward heat current when the temperature gradient is reversed. In our case, for a positive temperature gradient $T_h \leqslant T_c$, we have

$$(\beta_c - \beta_h) J_h^{\rm ste}(-\Delta T) = I(-\Delta T) + \xi(-\Delta T). \tag{19}$$

From Eqs. (15) and (19), we obtain

$$\begin{aligned} &(\beta_c - \beta_h)|J_h^{\rm ste}(\Delta T) + J_h^{\rm ste}(-\Delta T)| \\ =\ &|I(\Delta T) - I(-\Delta T) + \xi(\Delta T) - \xi(-\Delta T)|. \end{aligned} \tag{20}$$

Notice that Eq. (20) is achieved in the weak coupling limit, and in this case the term $\xi(\Delta T) - \xi(-\Delta T)$ is a small perturbation. Thus, Eq. (20) can be rewritten approximately as

$$(\beta_c - \beta_h)|J_h^{\rm ste}(\Delta T) + J_h^{\rm ste}(-\Delta T)| = |I(\Delta T) - I(-\Delta T)|. \tag{21}$$

In order to observe the corresponding relation between thermal rectification and correlation, we define

$$R_I = \frac{|I(\Delta T) - I(-\Delta T)|}{\max(|(I(\Delta T)|, |I(-\Delta T)|)}, \tag{22}$$

which describes the spatial asymmetry of system–environment correlations, with temperature gradient ΔT. In Fig. 5 we show R_J and R_I as functions of δ and γ in (a) and (b), respectively, which is the weak-coupling regime with $\gamma_h = \pi/16$ and $\gamma_c = \pi/32$ (a), $\delta_h = \pi/16$ and $\delta_c = \pi/32$ (b). Similarly, we present R_J and R_I with a large-scale coupling in (c) and (d). As expected, R_J and R_I are highly consistent in the weak-coupling case ((a) and (b)). In other words, the correlation and heat rectification can also witness each other. However, this corresponding relation is destroyed for a large-scale coupling ((c) and (d)).

5. Conclusion

In this paper we investigate the heat transport through a qubit open quantum system which is in contact with two hierarchical environments at different temperatures. Using a collision model approach, we manipulate the couplings between the system and the hierarchical environments and intraenvironment couplings, implementing dynamics with memory effects. We focus on the heat flux and correlations arising in NESSs. We demonstrate that the correlation can be regarded as the witness of a steady-state heat flux in the weak coupling limit, and their connections hold for heat rectification. The witness between heat flux (or rectification) and the correlations is verified through numerical calculations in the weak coupling regime. In addition, the monotonicity of the steady heat flux depends on whether the dynamics are Markovian or not in the weak coupling case.

Our paper shows that memory effects, which are often studied in the context of dynamical phenomena, have a connection with the steady-state heat flux and correlations. We expect that the properties revealed in this paper can help one to gain some insight into the role of the memory effect on the heat transport in NESSs, and may inspire more work in investigating the non-Markovianity in NESSs.

Appendix A

As the evolution in our model proceeds in discrete steps, we will employ the discretized version of the non-Markovianity measure, which is obtained as[61,62]

$$\mathcal{N} = \max \sum_{n \in \sigma^+} [D(\rho_{1,n+1}, \rho_{2,n+1}) - D(\rho_{1,n}, \rho_{2,n})], \tag{A1}$$

with $\sigma^+ = \bigcup_n (n, n+1)$ being the union of all the interaction steps $(n, n+1)$ within which $D(\rho_{1,n+1}, \rho_{2,n+1}) - D(\rho_{1,n}, \rho_{2,n}) > 0$, and $\{\rho_{1,n+1}, \rho_{2,n+1}\}$ are a pair of states of systems obtained starting from the corresponding pair of orthogonal states $\{|\psi_+\rangle, |\psi_-\rangle\}$ after $n+1$ steps of our protocol,

$$|\psi_+\rangle = \cos\frac{\theta}{2}|0\rangle + {\rm e}^{{\rm i}\varphi} \sin\frac{\theta}{2}|1\rangle,$$

$$|\psi_-\rangle = \sin\frac{\theta}{2}|0\rangle - \mathrm{e}^{\mathrm{i}\varphi}\cos\frac{\theta}{2}|1\rangle, \tag{A2}$$

where $\theta \in [0, \frac{\pi}{2}]$ and $\varphi \in [0, 2\pi]$. The maximization in Eq. (A1) is performed over all possible values of θ and φ, i.e., all possible orthogonal pairs of initial system states. In Fig. A1, we show the relationship between steady heat flux and non-Markovianity with different temperature differences between two reservoirs, specifically with small temperature difference $\Delta T = 0.01$ and large temperature difference $\Delta T = 10$ in Figs. A1(a) and A1(b), respectively. This shows that the maximum value of heat flux is at the boundary of Markovian and non-Markovian in the weak-coupling region, which is insensitive to the temperature difference between the two reservoirs.

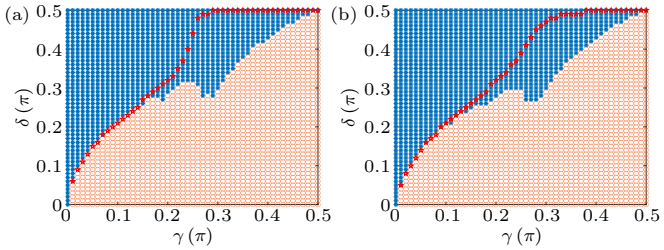


Fig. A1. The exhibition of the maximum value of the steady heat flux (red five-pointed star) in Markovian and non-Markovian regions with different temperature differences between the two reservoirs. (a) A small temperature difference with $T_h = 1.01$ and $T_c = 1$; (b) a large temperature difference with $T_h = 10$ and $T_c = 1$. For both plots $|\psi\rangle_S = |1\rangle$ and $k_B = \omega = 1$.

Acknowledgements

This paper is financially supported by the National Natural Science Foundation of China (Grant No. 12465005) and the Natural Science Foundation of Inner Mongolia Autonomous Region of China (Grant No. 2024MS01018).

References

[1] Gemmer J, Michel M and Mahler G 2004 *Quantum Thermodynamics: Emergence of Thermodynamic Behavior Within Composite Quantum Systems* (Berlin: Springer)
[2] Binder F, Correa L A, Gogolin C, Anders J and Adesso G 2018 *Thermodynamics in the Quantum Regime: Fundamental Aspects and New Directions, Fundamental Theories of Physics* (Cham: Springer International Publishing)
[3] Esposito M, Harbola U and Mukamel S 2009 *Rev. Mod. Phys.* **81** 1665
[4] Deffner S and Lutz E 2011 *Phys. Rev. Lett.* **107** 140404
[5] Taylor E and Segal D 2015 *Phys. Rev. Lett.* **114** 220401
[6] Purkayastha A, Dhar A and Kulkarni M 2016 *Phys. Rev. A* **93** 062114
[7] Landi G T, Poletti D and Schaller G 2022 *Rev. Mod. Phys.* **94** 045006
[8] Talkner P, Lutz E and Hänggi P 2007 *Phys. Rev. E* **75** 050102
[9] Horodecki M and Oppenheim J 2013 *Nat. Commun.* **4** 2059
[10] Alicki R and Fannes M 2013 *Phys. Rev. E* **87** 042123
[11] Alicki R 1979 *J. Phys. A: Math. Gen.* **12** L103
[12] Campisi M, Talkner P and Hänggi P 2009 *Phys. Rev. Lett.* **102** 210401
[13] Anders J and Giovannetti V 2013 *New J. Phys.* **15** 033022
[14] Ankerhold J and Pekola J P 2014 *Phys. Rev. B* **90** 075421
[15] Pyhäranta T, Alipour S, Rezakhani A T and Ala-Nissila T 2022 *Phys. Rev. A* **105** 022204
[16] Holdsworth T and Kawai R 2022 *Phys. Rev. A* **106** 062604
[17] Lipka-Bartosik P, Diotallevi G F and Bakhshinezhad P 2024 *Phys. Rev. Lett.* **132** 140402
[18] Partovi M H 2008 *Phys. Rev. E* **77** 021110
[19] Jennings D and Rudolph T 2010 *Phys. Rev. E* **81** 061130
[20] Micadei K, Peterson J P S, Souza A M, Sarthour R S, Oliveira I S, Landi G T, Batalhão T B, Serra R M and Lutz E 2019 *Nat. Commun.* **10** 2456
[21] Plenio M B and Virmani S 2007 *Phys. Rev. Lett.* **99** 120504
[22] Benenti G, D'Arrigo A and Falci G 2009 *Phys. Rev. Lett.* **103** 020502
[23] Caruso F, Giovannetti V and Palma G M 2010 *Phys. Rev. Lett.* **104** 020503
[24] Caruso F, Giovannetti V, Lupo C and Mancini S 2014 *Rev. Mod. Phys.* **86** 1203
[25] Palafox S, Román-Ancheyta R, Çakmak B and Müstecaplıoğlu E 2022 *Phys. Rev. E* **106** 054114
[26] Lorenzo S, Farace A, Ciccarello F, Palma G M and Giovannetti V 2015 *Phys. Rev. A* **91** 022121
[27] Lorenzo S, McCloskey R, Ciccarello F, Paternostro M and Palma G 2015 *Phys. Rev. Lett.* **115** 120403
[28] Pezzutto M, Paternostro M and Omar Y 2016 *New J. Phys.* **18** 123018
[29] Ptaszyński K and Esposito M 2019 *Phys. Rev. Lett.* **123** 200603
[30] Purkayastha A, Guarnieri G, Campbell S, Prior J and Goold J 2021 *Phys. Rev. B* **104** 045417
[31] Ask A and Johansson G 2022 *Phys. Rev. Lett.* **128** 083603
[32] Heineken D, Beyer K, Luoma K and Strunz W T 2021 *Phys. Rev. A* **104** 052426
[33] Senior J, Gubaydullin A, Karimi B, Peltonen J T, Ankerhold J and Pekola J P 2020 *Commun. Phys.* **3** 40
[34] Gubaydullin A, Thomas G, Golubev D S, Lvov D, Peltonen J T and Pekola J P 2022 *Nat. Commun.* **13** 1552
[35] Segal D and Nitzan A 2005 *Phys. Rev. Lett.* **94** 034301
[36] Wu L A and Segal D 2009 *Phys. Rev. Lett.* **102** 095503
[37] Bermudez A, Bruderer M and Plenio M B 2013 *Phys. Rev. Lett.* **111** 040601
[38] Kato A and Tanimura Y 2015 *J. Chem. Phys.* **143** 064107
[39] Medina González P U, Ramos-Prieto I and Rodríguez-Lara B M 2020 *Phys. Rev. A* **101** 062108
[40] Ciccarello F, Lorenzo S, Giovannetti V and Palma G M 2022 *Phys. Rep.* **954** 1
[41] Campbell S and Vacchini B 2021 *Europhys. Lett.* **133** 60001
[42] Deffner S and Campbell S 2019 *Quantum Thermodynamics* (Williston: Morgan & Claypool Publishers)
[43] Myers N M, Abah O and Deffner S 2022 *AVS Quant. Sci.* **4** 027101
[44] Vinjanampathy S and Anders J 2016 *Contemp. Phys.* **57** 545
[45] De Chiara G, Landi G, Hewgill A, Reid B, Ferraro A, Roncaglia A J and Antezza M 2018 *New J. Phys.* **20** 113024
[46] Li L, Zou J, Li H, Xu B M, Wang Y M and Shao B 2018 *Phys. Rev. E* **97** 022111
[47] Khandelwal S, Palazzo N, Brunner N and Haack G 2020 *New J. Phys.* **22** 073039
[48] Pellegrini C and Petruccione F 2009 *J. Phys. A: Math. Theor.* **42** 425304
[49] Filippov S N, Piilo J, Maniscalco S and Ziman M 2017 *Phys. Rev. A* **96** 032111
[50] Beyer K, Luoma K and Strunz W T 2018 *Phys. Rev. A* **97** 032113
[51] Li Y W and Li L 2021 *EPJ Quantum Technol.* **8** 9
[52] Kretschmer S, Luoma K and Strunz W T 2016 *Phys. Rev. A* **94** 012106
[53] Campbell S, Ciccarello F, Palma G M and Vacchini B 2018 *Phys. Rev. A* **98** 012142
[54] Man Z X, Xia Y J and Lo Franco R 2019 *Phys. Rev. A* **99** 042106
[55] Scarani V, Ziman M, Štelmachovič P, Gisin N and Bužek V 2002 *Phys. Rev. Lett.* **88** 097905
[56] Nielsen M A and Chuang I L 2000 *Quantum Computation and Quantum Information* (Cambridge: Cambridge University Press)
[57] Cerf N J and Adami C 1998 *Phys. D* **120** 62
[58] Ordonez-Miranda J, Ezzahri Y and Joulain K 2017 *Phys. Rev. E* **95** 022128
[59] Li N, Ren J, Wang L, Zhang G, Hänggi P and Li B 2012 *Rev. Mod. Phys.* **84** 1045
[60] Joulain K, Ezzahri Y, Drevillon J and Ben-Abdallah P 2015 *Appl. Phys. Lett.* **106** 133505
[61] Laine E M, Piilo J and Breuer H P 2010 *Phys. Rev. A* **81** 062115
[62] Vacchini B 2012 *J. Phys. B: At. Mol. Opt. Phys.* **45** 154007